TD-99-012
March 26, 1999

Design Study of 45-mm Bore Dipole Magnet for 11 to 12 Tesla Field

Ryuji Yamada & Jonathan Moeller, Fermilab
Masayoshi Wake, KEK

Summary

Two designs of 45-mm bore dipole magnets are described about their magnetic characteristics. The first one has a 25-mm thick collar with overall diameter of 520 mm. The other one has a 9-mm thin spacer with the overall diameter of 434 mm. Both of them have good field regions of 10^{-4}, 28 mm wide horizontally and 24 mm wide vertically. With further adjustment of higher harmonics, the good field region can be horizontally increased to 33 mm. With the installation of a beam screen, the estimated vacuum space available for the beam operation is 33 mm wide horizontally and 22 mm wide vertically. If we assume that the total degradation of short sample data is 18.5%, the maximum central field values at quench current will be between 11.3 and 11.5 T.

I. Introduction

For the next couple of years we have to make several one-meter long model magnets at Fermilab. We have to develop Nb_3Sn high field dipole magnets in the magnetic field strength in the range from 11 to 12 T, for a Very Large Hadron Collider (VLHC). We should aim to start building practical accelerator-type prototype magnets with reasonable operational apertures, which lead to the production-type magnets for VLHC.

There are two following major items to be considered.

1. Magnet Cross Section and its Magnetic Calculation
2. Mechanical Structure

In this report only the first item is discussed and the second item will be reported in a separate note.

As the first prototype one-meter magnet we propose to make a magnet with a 45-mm bore and with a rather conventional collar structure, because we should like to establish timely production experiences at Fermilab. We should also begin work on the second and third design.

We should compare the proposed 45-mm bore design with the other 40-mm bore design [1,2] and the 50-mm bore design [3,4] for their advantages and disadvantages.

II. Magnet Cross Section Design

The cross section of the magnet with 45-mm bore with a 25-mm thick collar and with the overall diameter of 520 mm is shown in Figure 1. The cosine-θ type coil is wound in two layers using the same cable to avoid the splicing of the conductors inside the high field region. Thus the inner and outer half coils are wound with the same cables as shown in Fig. 2. The major parameters of this 45-mm bore design are listed in Table I.

Another design with a 9-mm thin spacer has the overall diameter of 434 mm, and its major parameters are listed also in Table I.

There are two cases that we study magnetically and discuss in this report. For the mechanical structure we report only one, which is designed with a rather conventional collar for the coil. The coil is clamped and preloaded with a thick stainless steel collar. It is done with the familiar method traditionally used with superconducting dipole magnets at Fermilab. Then the coil with collared structure is clamped with a vertically split iron yoke with aluminum spacers at the top and bottom edges. The whole outside surface is covered with the top and bottom half circle stainless steel skin and welded together under compression.

III. Superconductor Strand and Cable

Presently, Nb_3Sn is the most viable and commercially available superconducting material for high field magnets in the 10 to 13 T operational field range. It has been actively developed for the fusion project with the aim of producing a conductor with smaller AC loss and with medium-high current density. For high energy accelerator and collider application, we need a superconductor strand with J_c of above 2200 A/mm^2 at 4.2 K and 12 T with the effective filament size of 20 μm or less. We do not have such a material commercially available yet, but it seems it will be available in a few years.

There are several different possible methods to produce Nb_3Sn superconductors for our application. Presently we are buying Nb_3Sn conductor from IGC, made with the Internal Tin method. The modified jelly roll type conductor from Oxford Instruments Inc. can have a current density of about 2000 A/mm^2 at 4.2 K and 12 T, but with a D_{eff} value of 70 μm or more. Recently, Shape Metal Innovation BV has been producing superconductor with the PIT method capable of 1600 A/mm^2 at 4.2 K and 12 T with a smaller D_{eff} value of 20 μm [5]. Another big advantage of this material is its very short reaction time of 100 hours, compared to others with 500 hours or more.

The major specification parameters for our present conductor, FNAL specification #5520-ES-362049, are shown in Table II together with preferred values for future application. The first shipment of the specified strand from IGC was delivered on the March 12, 1999, and its measured characteristic parameters will be reported in a month.

Table II. Major specification parameters of the superconducting strand

Items	Units	Specifications	Preferred Values for Future Ordering
Diameter	mm	1.00	
J_c at 4.2 K	A/mm^2		
At 12 T		> 1886	> 2200
(at 13 T)		(> 1435)	
I_c at 12 T at 4.3 K	A	> 800	
Cu/SC ratio	%	46	
D_{eff}	μm	< 70	< 20
RRR of Copper		>75	>100
Reaction Time	hour	(~600)	>100

The superconducting cable for the 45-mm bore design will be made of 28 strands and with a cabling angle of 14.5 degrees. The cable is compacted and key-stoned, with 1.0 degree key-stone angle. Its bare width without insulation is 14.238 mm, and its median height is 1.785 mm. The overall cross-section with insulation is shown in Figure 2. Its overall width with insulation is 14.538 mm, and its narrow and thick edges have heights of 1.901 mm and 2.149 mm respectively. Its radial and azimuthal insulation thicknesses are 0.15 mm and 0.12 mm respectively.

The packing factor of the cable will be about 91%. The degradation of the J_c value of the strand due to the cabling operation is expected to be about 88% [6]. The further degradation of the J_c value of the Nb_3Sn conductor has been studied and estimated with past Nb_3Sn magnets with regard to the compressive loading of the Lorentz force. The past reported results were not consistent, and depended on the individual magnet. The latest data from University of Twente group show the following results for PIT conductor [7]. The degradation of the normalized critical current $I_c(\sigma)/I_c(0)$ of a completely epoxy-filled Nb_3Sn cable due to the transverse strain σ can be described by the following formula.

$$I_c(\sigma)/I_c(0) = 1.00 - 2.50 \times 10^{-4}\sigma - 3.95 \times 10^{-6}\sigma^2$$

where σ is given in units of MPa. According to this formula, the critical current will degrade to 2.2%, 6.5%, 10%, and 12.6% at the strain σ of 50, 100, 130, and 150 MPa [7].

IV. Design of Coil Configuration using ROXIE

The detailed coil configuration is optimized first by using ROXIE v4.4 [8], which does not have the capability for calculating the effect of iron yoke saturation. The use of the ROXIE program aims to optimize the configuration of the conductor blocks for the following purposes:

- To make the usable good field region ($dB/B_0 < 10^{-4}$) as wide as possible.
- To make all higher harmonic components as small as possible (for good round aperture).
- To make the center pole width as wide as possible for ease of winding cables.

The results of the two ROXIE calculations, which used a magnetic permeability value of 1000, are shown in Fig. 3a and 3b. Both cases are calculated using the cable configuration shown in Figure 2. Their main difference is in the values of inner radius of the yoke iron. The first case in Fig. 3a is calculated with a smaller iron I.R. value of 60.5 mm with a thin spacer of 8.64 mm. It corresponds to the case where the yoke is placed close to the coil using a thin aluminum spacer between the coil and yoke to maximize the ultimate central magnetic field value with a smaller excitation current.

The second case in Figure 3b is designed for a magnet assembled with a thick collar of 25 mm and iron I.R. of 77.5 mm. In this case, the contribution of the iron yoke for the central field value is reduced, but has a little better iron saturation effect. The maximum field value in the coil occurs at the inner corner of the innermost current block. Its

magnetic field value is 5.1% over the central field value $B_y(0)$. Major parameters of these two cases are shown in Table III.

In both cases, the good field regions show almost the same patterns as in Figures 3a and 3b. For the good field region of 1.0×10^{-4}, the total horizontal width is 28.0 mm for both cases. The total vertical height is 24.4 mm for the thin spacer magnet and 24.0 mm for the thick collar case. If we need a horizontally wider good field region, we could choose a conductor configuration with $b_9 \approx -0.17$ or $b_{11} \approx 0.0$. Then we could make the horizontal good field region wider by 5 mm. This method will be reported separately.

The maximum short sample central field obtained using ROXIE is 12.4 T at 16.8 kA for the thin-collared magnet and 12.2 T at 18.3 kA for the thick-collared magnet. The difference in the maximum central field values is only 0.2 T, but the difference in the current value of 1.5 kA is quite big due to the difference in the iron yoke contribution.

V. Magnetic Field Calculation using ANSYS

After the coil configuration is optimized with the ROXIE program, its geometric parameters are transferred into the ANSYS v5.5 program [9]. In ANSYS, the coordinates of the four corners of each cable are defined as in ROXIE. The geometric coordinates of the yoke including its inside and outside radii are defined, and a real B-H curve is used to calculate the saturation effect of the iron [10].

First, the data calculated with ANSYS at each excitation current are used to calculate the field distribution $B_y(x)$ on the median plane and displayed with the program EXCEL, as shown in Figure 4. Then the radial field data $B_r(r = 1\text{cm}, \theta)$ are calculated on an arc of 1-cm radius for 49 points with equal spacing using ANSYS data. These data are used to calculate the harmonic components, from b_3 to b_{13}, using the program TRICOF [11]. These harmonic data sets are now displayed in chart form using EXCEL [10].

The harmonics distributions from b_3 to b_{13} are shown in Fig. 5a for the magnet with 25 mm collar and with no special holes for the correction of the iron saturation effect. It shows that the value of b_3 changes drastically due to the inhomogeneous saturation on the inside surface of yoke beyond 10 kA. It is interesting to note that the other harmonic components are fairly constant over the whole range. These values are much bigger than those calculated by ROXIE, but they are still below 0.4×10^{-4}.

VI. Correction of Iron Saturation Effect Using Holes in Yoke

In order to reduce the variation of sextupole term b_3, a set of holes are introduced in the yoke [12,13]. Without the holes, the top and bottom inner surfaces of the yoke start to saturate strongly. Some of the small holes are placed near the side surfaces of the yoke so that the whole iron surface starts to saturate more uniformly.

The geometry of the 25 mm collared magnet with yoke holes is shown in Figure 7, where we can observe the flux distribution around the holes. The $B_y(x)$ field distribution on the median plane is shown in Figure 4 for this 25 mm collared magnet with holes at 1, 7.5, 13, and 18 kA excitation. The resulting distributions of the harmonics with respect to the current excitation values are shown in Figure 5b. It shows that the sextupole term b_3 is greatly improved with the addition of these holes in the yoke. Its maximum

variation is within about 1.6 10^{-4} scale units, which could be reduced further with more adjustment.

The excitation curve of the magnets are shown in Figure 6a, where the central field B_0 is plotted vs. excitation current with and without holes. It shows that the addition of the holes in the yoke reduces the transfer function. The central field value of the 25 mm collared magnet at 18 kA is now reduced to 11.27 T from 11.48 T without holes. With the 9 mm thin spacer the corresponding values changed from 11.87 T to 11.47 T with holes.

VII. Forces and Stresses on the Conductors

The forces and stresses on the inner and outer layers, calculated at 11 T with ROXIE and ANSYS for both types of magnets, are listed in Table IV. The azimuthal forces are totaled in the inner and outer layers individually and their corresponding stress values in the midplane are listed as P_{in} and P_{out}. Because the azimuthal forces are totaled assuming no friction, these stress values are upper limits. The estimated necessary preload P_{pre} is also given for some of the cases. The midplane stress values are higher for the cases calculated using ANSYS. This is due to increased current from the iron saturation effect.

VIII. Maximum Central Field Strength

The possible maximum central field values of the 45-mm bore magnet are calculated successively and shown in Table III. These calculations assume a current density of 1886 A/mm^2, which is more like I_c of 800 A/strand at 12 T. Our estimations also assume that there is no degradation due to the cabling and keystoning operations or from compressive Lorentz forces.

First, the central field is estimated by using ROXIE with a constant permeability of 1000. The maximum central field $B_y(0)$ with short sample data obtained in these cases are 12.4 and 12.2 T for the thin- and thick-collared magnets, respectively. In these cases the peak field in the coil is 5.1% higher than the central field $B_y(0)$.

Then the maximum central field is estimated with ANSYS, using the detailed input data file of ROXIE. In this case the magnetic field is calculated with a realistic B-H curve. The cases are run with and without holes in the yoke. The load lines and the peak field lines in the coil, which are assumed to be 6.3% higher than the central values, are shown in Figure 6b for the 9 mm thin spacer design and also in Figure 6c for the 25 mm collared design. To estimate the maximum attainable field values, the short sample data for the conductor cables are shown with degradation factors of 100%, 90%, and 80%.

Without any degradation in the cable current density, the maximum central field values of the 9 mm spacer design are 12.0 T without holes and 11.9 T with holes. In the 25 mm collared design, these values are 11.9 T and 11.83 T respectively. We must, however, mention that all of these field values require excitation currents above 18 kA, which exceeds the limit of our present power supply.

If we assume a 12% cabling degradation factor and the degradation due to the transverse stress is 6.5% at 100 MPa, then the overall degradation factor will be 18.5%. Including the degradation effects, the maximum central field values can be estimated

from Figures 6b and 6c. For the 9 mm thin-spacer design, these values are 11.5 T without holes and 11.4 with holes. The corresponding values for the 25 mm collared design are 11.4 T and 11.3 T. Fortunately, these values are just attainable with our present 18 kA power supply, but we will eventually need a 20 kA or higher power supply.

IX. Considerations for Beam Screen and Vacuum

In the LHC Design Report, it is estimated that each beam will emit synchrotron radiation with a power of 0.206 W/m/ring. It is also estimated that there is a similar amount of the resistive beam loss in the beam tube, totaling about 0.5 W/m/ring for the luminosity of $1.0 \times 10^{34}/cm^2/s$ [14]. These values are excessive heat load for the LHC's 1.9 K cooling system. Thus the so-called beam screen is inserted inside the magnet cold bore to intercept this power. The beam screen is maintained at a temperature between 5 K and 20 K by gaseous helium flow.

For the 50-50 TeV p-p VLHC, the synchrotron radiation power emitted in the vacuum tube is about 6 W/m/ring for the designed luminosity of $1.0 \times 10^{34}/cm^2/s$ [15]. Therefore we need about 12 times more powerful cooling power for the VLHC beam screen. We have to design and study such a beam screen and its effect on the vacuum. Its delicate structure becomes increasingly more difficult with the smaller bore size, and the vacuum situation is getting worse with the smaller bore size. Without these problems solved, we cannot decide the real bore size of the magnet.

The proposed geometries of the beam screens for different sized magnets are shown in Figure 8. Within the bore diameter of 45-mm, we have to put a vacuum tube of 41 mm O.D. and 39 mm I.D. There is a 2 mm thick annular area, for the liquid helium cooling the coil and supporting the vacuum tube. Then the beam screen is mounted inside the vacuum tube. The beam screen will be made of 1 mm thick perforated stainless steel pipe, with two cooling tubes welded on the top and bottom. Its horizontal inside width will be 33 mm and vertical inside height will be 22 mm. The space between the beam screen and vacuum tube is 2 mm around, which is used for the mechanical support of the beam screen. Regardless of the bore size, we need about 12 mm of the total horizontal bore width for placing the beam screen and vacuum tube.

As mentioned before, the good field region is +/- 14 mm horizontally and +/- 12 mm vertically. Therefore the good field region just fits inside the horizontal width of the beam screen of 33 mm, but vertically it is cropped to 22 mm, losing an additional 2 mm of height.

The interrelations among the synchrotron radiation, the beam screen dimensions, and the inside vacuum are complicated and should be studied in detail. They will affect the decision of the selection of the bore size of the magnet.

X. Effect from Magnetization

The present superconducting strand is estimated to have an effective diameter D_{eff} on the order of 70 μm. It has quite a big magnetization, and its persistent current is going to influence the injection field quite strongly. Its magnitude of the sextupole and decapole

was calculated by T. Ogitsu for the 50-mm bore size, and is shown in Figure 9. The nominal injection field for the 50-50 TeV Collider is 0.72 T for the 3 TeV injection beam. The sextupole hysteresis is about 80 in 10^{-4} unit. The important thing is if it is such a big value, then the fluctuating values in the mass produced conductors will have quite a variation in their magnetization value. We have to ask the superconductor industry to develop a superconductor with an effective diameter about ten times smaller.

XI. Accelerator-Related Problems, Closed Orbit Distortion, and Alignment Errors

There are other accelerator-related problems that should be solved before the exact dimensions of bore size should be chosen. These are related to the beam dynamics. How much the beam will deviate from the central orbit due to the field errors caused by higher harmonics components, including the effect of persistent current at injection time? How big the closed orbit distortion might be due to the misalignment errors of the quadrupole magnets? We have to do extensive and detailed beam tracking calculation. These issues should be addressed separately.

XII. Conclusions

With the present 45-mm magnet bore design, we can build an 11 T high field magnet, with good field quality and sound mechanical structure, and with a reasonably wide aperture.

The magnetic field quality can be made satisfactorily. The good field region with 1.0×10^{-4}, is 28 mm wide horizontally and 24 mm wide vertically. This width can be increased to approximately 33 mm with further adjustment of higher geometric harmonics. With a tentative beam screen installed, the usable vacuum space is 33 mm horizontally and 22 mm vertically. With a more realistic beam screen design, possibly with bigger cooling tubes, the usable space might become more restricted.

The center pole of the collar is made 16 mm wide at its bottom. With this dimension, we can wind the 28-strand cable conductor made of 1 mm strand, around the center pole. The compressive force for the conductor is also reasonable.

There are a lot of things to be worked out yet. We have to design and develop a reliable beam screen to cool the power of 6 W/m synchrotron radiation, and make a good vacuum system. We have to know more about beam dynamics. Moreover we have to work with industry to develop greatly improved superconductor.

References

[1]. V.V. Kashikhin and I. Terechkine, "40-mm Bore Dipole Cross-Section Using Cable Made of 1-mm-Diameter Nb_3Sn Strand." TD-99-014, March 4, 1999.
[2]. G. Ambrosio and V.V. Kashikhin , "40-mm Bore HFM Cross-Section design with 0.8 mm Strand Diameter Nb_3Sn Cable." TD-99-10, FNAL, March 1999.
[3]. S. Caspi and M. Wake, " A 12 Tesla Dipole for VLHC". LBNL Preprint SC-MAG-635, Dec. 16, 1998.
[4]. M. Wake, "Conceptual Design of Nb_3Sn High Field Dipole Magnet." KEK internal 98-3, July 1998.
M. Wake, "Conceptual Design Update of Nb_3Sn High Field Dipole Magnet." TD-99-009, FNAL, March 1998.
[5] "The hard facts of the "Powder in Tube' conductor", Shape Metal Innovation BV
[6]. E. Barzi, "I_c Degradation due to Cabling in Internal Tin Nb_3Sn." TD-99-006, FNAL, February 1999.
[7] H. ten Kate, "Recent developments on PIT Nb_3Sn conductors". High Field Accelerator Magnets Workshop, Erice, March 12, 1999.
[8]. S. Russenchuck, " A Computer Program for the Design of Superconducting Accelerator Magnets." CERN AT/95-39, LHC Note 354, September 26, 1995.
[9]. ANSYS. Finite Element Analysis program from SAS, Inc.
[10]. J. Moeller, " ANSYS Procedure for 2D Field Analysis and Iron Saturation Study." TD-99-016, March 1999.
[11]. Harm.exe, executable form of TRICOF harmonic analysis procedure. It was extracted from ROXIE fortran source by V. Kashikhin.
[12]. R. Gupta et. al. "Field Quality Control Through the Production Phase of RHIC Arc Dipoles." Proceedings of 1995 PAC and International Conference on High Energy Accelerators. p. 1423
[13]. R. Yamada and J. Moeller, "Saturation Effect and Field Correction using Holes in Yoke." TD-99-017, March 1999.
[14]. The LHC Study Group, "LHC: The Large Hadron Collider Conceptual Design". CERN/AC/95-05 (LHC), October 20, 1995.
[15]. M.J. Syphers "High Field Approaches to 100 TeV Hadron Colliders." Accelerator Physics Issues in Future Hadron Colliders, Session I. Mini-Symposia, 1998 Annual Meeting of APS.

Table I. Major Parameters of 45-mm I.D. Coil Magnet

Item	Units	25 mm Collar	9 mm Spacer
I.D. of Coil	mm	45	45
I.D. of Vacuum Tube	mm	39	39
Usable Region with Beam Scr.			
Full Width	mm	33	33
Full Height	mm	22	22
Good Field Region $< 10^{-4}$			
Full Width	mm	28	28
Full Height	mm	24	24.4
Strand Diameter	mm	1.0	1.0
Cable			
No. of Strands in Cable		28	28
Bare Cable Width	mm	14.238	14.238
Bare Cable median Height	mm	1.785	1.785
Keystone Angle	deg	1.0	1.0
Radial Insul. Thick.	mm	0.15	0.15
Azimuthal Insul. Thick.	mm	0.12	0.12
No. of Turns		30 x 2	30 x 2
No. of Layers		2	2
No. of Current Blocks		3 + 3	3 + 3
Collar Thickness	mm	25	8.64
Collar Material			
Iron Yoke I. R.	mm	77.5	60.5
Iron Yoke O.R.	mm	253	210
Skin Thickness	mm	7	7
Magnet O.R.	mm	260	217
Magnet O.D.	mm	520	434
I_{max} at 100% S.S.	A	18800	18300
B_{max} at 100% S.S.	T	11.9	12.0
I_{max} at 81.5% S.S.	A	17800	17300
B_{max} at 81.5% S.S.	T	11.4	11.5

Table III. Major magnetic field parameters of two different configurations of the magnet.

Item	Units	Thin Collar	25 mm Collar	Thin Collar	25 mm Collar	Thin Collar	25 mm Collar
Correspond to		Fig. 3a	Fig. 3b				Fig.7
Program		ROXIE	ROXIE	ANSYS	ANSYS	ANSYS	ANSYS
With Holes				No	No	Yes	Yes
No. of Turns		60	60	60	60	60	60
Collar	mm	8.64	25	8.64	25.5	8.64	25.5
Yoke I.R.	mm	60.5	77.0	60.5	77.5	60.5	77.5
Yoke O.R.	mm			210	253	210	253
Skin Thickness	mm			7	7	7	7
Magnet O.D.	mm			217	260	217	260
Pole Width	mm	15.9	16.0	15.9	16.0	15.9	16.0
Usable Region							
Total Width	mm	28.0	28.0				
Total Height	mm	24.4	24.0				
Permeability		1000	1000	B-H	B-H	B-H	B-H
I @ 11 T	A	14850	16631	16400	17100	17130	17550
Stored Energy	kJ/m	256	279				
Inductance	mH/m	2.32	2.02				
At 100% S.S							
Quench I	A	16800	18300	18300	18760	18800	19100
$B_y(0)$ at Q	**T**	**12.4**	**12.2**	**12.0**	**11.9**	**11.9**	**11.84**
At 81.5% S.S							
Quench I	A			17300	17800	17800	18100
$B_y(0)$ at Q	**T**			**11.5**	**11.4**	**11.4**	**11.3**
Harmonics at 1-cm	10^{-4} unit				At 1 kA		
b_3		0.00033	0.00316		0.45		
b_5		-0.00003	0.00319		0.38		
b_7		-0.00142	-0.00081		-0.025		
b_9		-0.07328	-0.09007		0.2		
b_{11}		0.0738	0.08203		0.04		
b_{13}		-0.00092	-0.00076		0.18		

Table IV. Magnetic forces and stresses

Item	Units	Thin Collar	25 mm Collar	Thin Collar	25 mm Collar	Thin Collar	25 mm Collar
Correspond to		Fig. 3a	Fig. 3b				Fig.7
Program		ROXIE	ROXIE	ANSYS	ANSYS	ANSYS	ANSYS
With Holes				No	No	Yes	Yes
Collar	mm	8.64	25	8.64	25.5	8.64	25.5
Yoke I.R.	mm	60.5	77.0	60.5	77.5	60.5	77.5
Yoke O.R.	mm			210	253	210	253
Skin Thickness	mm			7	7	7	7
Magnet O.D.	mm			217	260	217	260
I @ 11 T	A	14850	16631	16400	17100	17130	17550
Stored Energy	kJ/m	256	279				
Forces @ 11 T							
F_x – inner	kN/m	1504	1621	1614	1646	1656	1685
F_x – outer	kN/m	954	794	849	752	756	714
F_x – total	kN/m	2458	2415	2463	2398	2412	2399
F_y – inner	kN/m	-196	-245	-248	-263	-260	-273
F_y – outer	kN/m	-653	-821	-838	-885	-875	-918
F_y – total	kN/m	-849	-1066	-1086	-1148	-1135	-1191
F_θ – inner	kN/m	-931	-1035	-1033	-1065	-1070	-1096
F_θ – outer	kN/m	-1068	-1153	-1181	-1189	-1185	-1207
F_θ – total	kN/m	-1999	-2188	-2214	-2254	-2255	-2303
Stress @ 11T							
P_{in} – midplane	MPa	65	64	73	75	75	77
P_{out} – midplane	MPa	75	73	83	83	83	85
Preload @ 11T							
P_{pre} - preload	MPa		51				

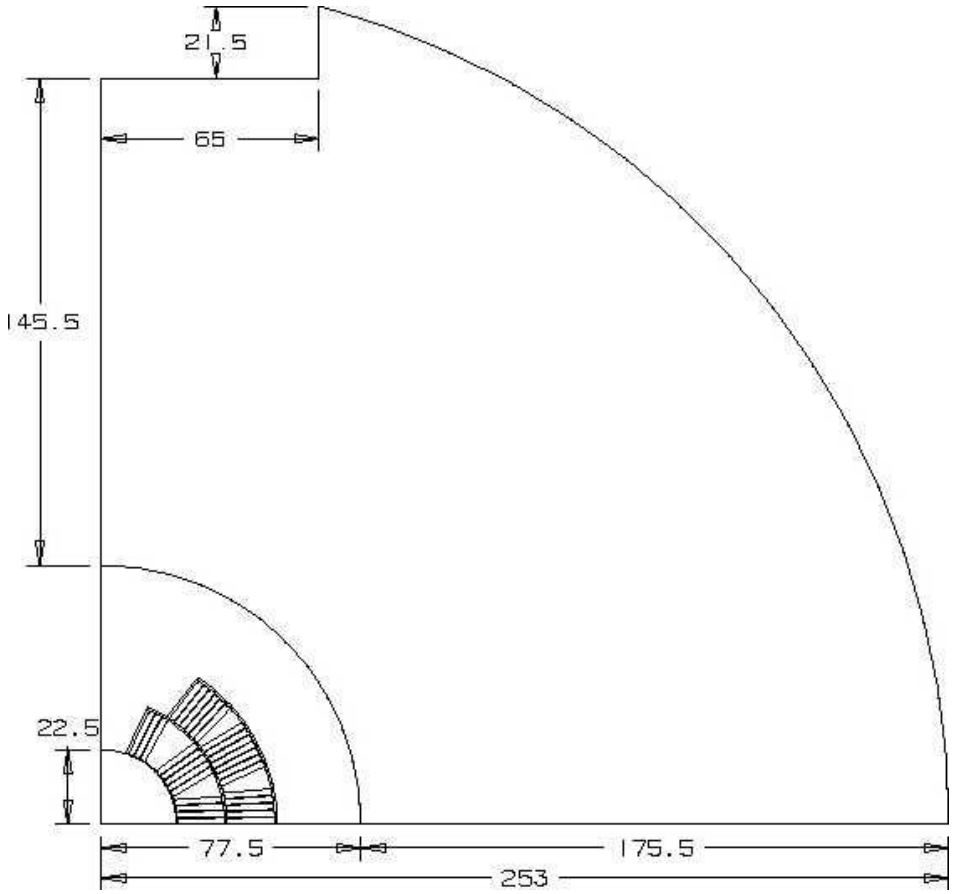

Figure 1. Dimensions of the 45-mm dipole coil and yoke [units in mm].

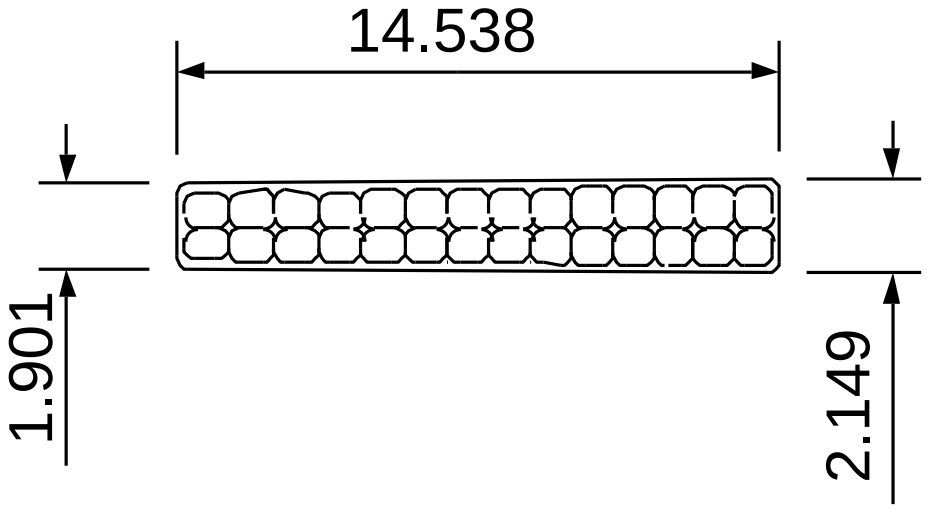

Figure 2. Dimensions of the insulated 28-strand cable [units in mm].

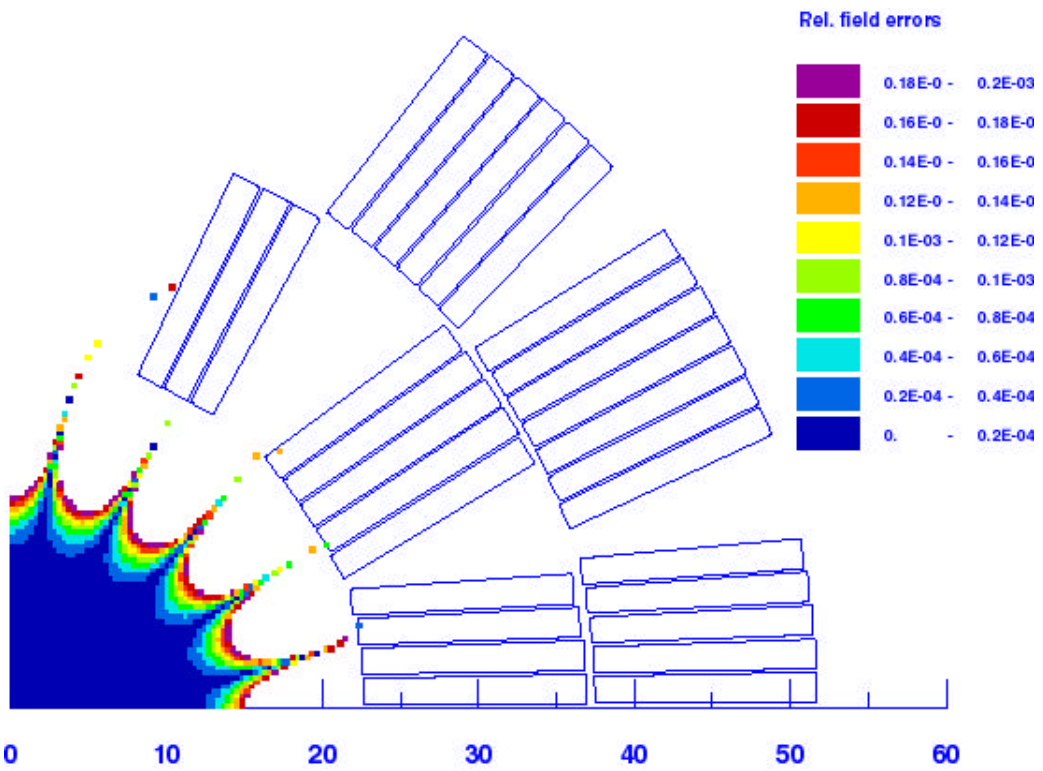

Figure 3a. ROXIE field quality with 9 mm collar.

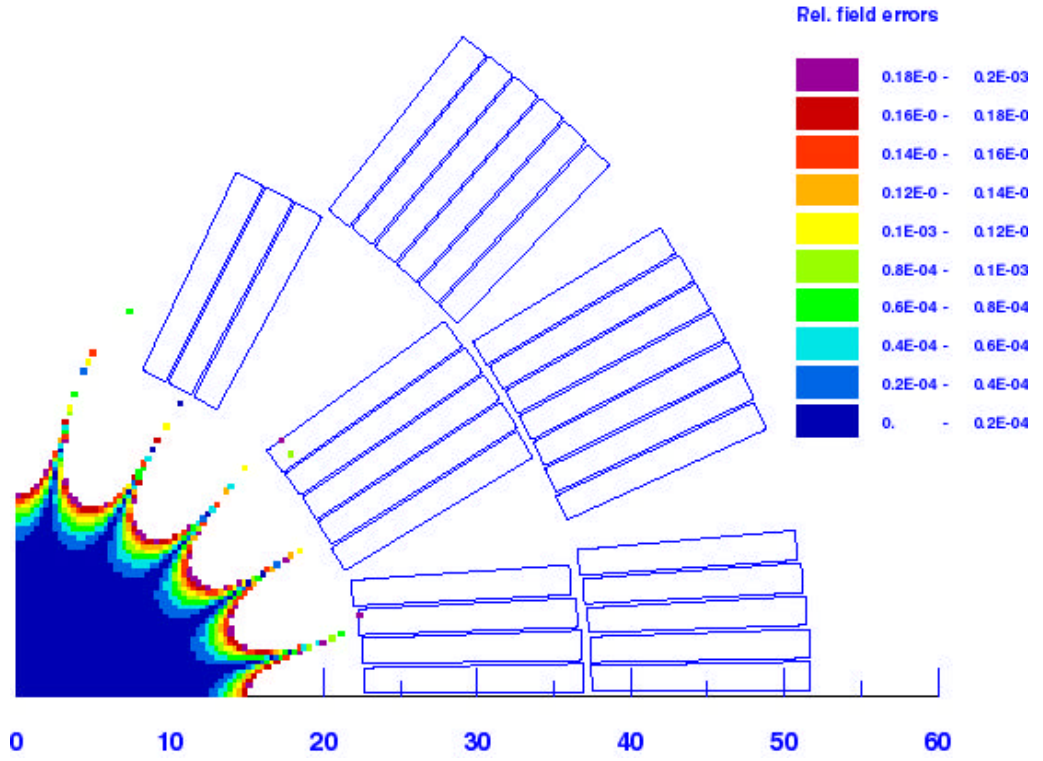

Figure 3b. ROXIE field quality with 25 mm collar.

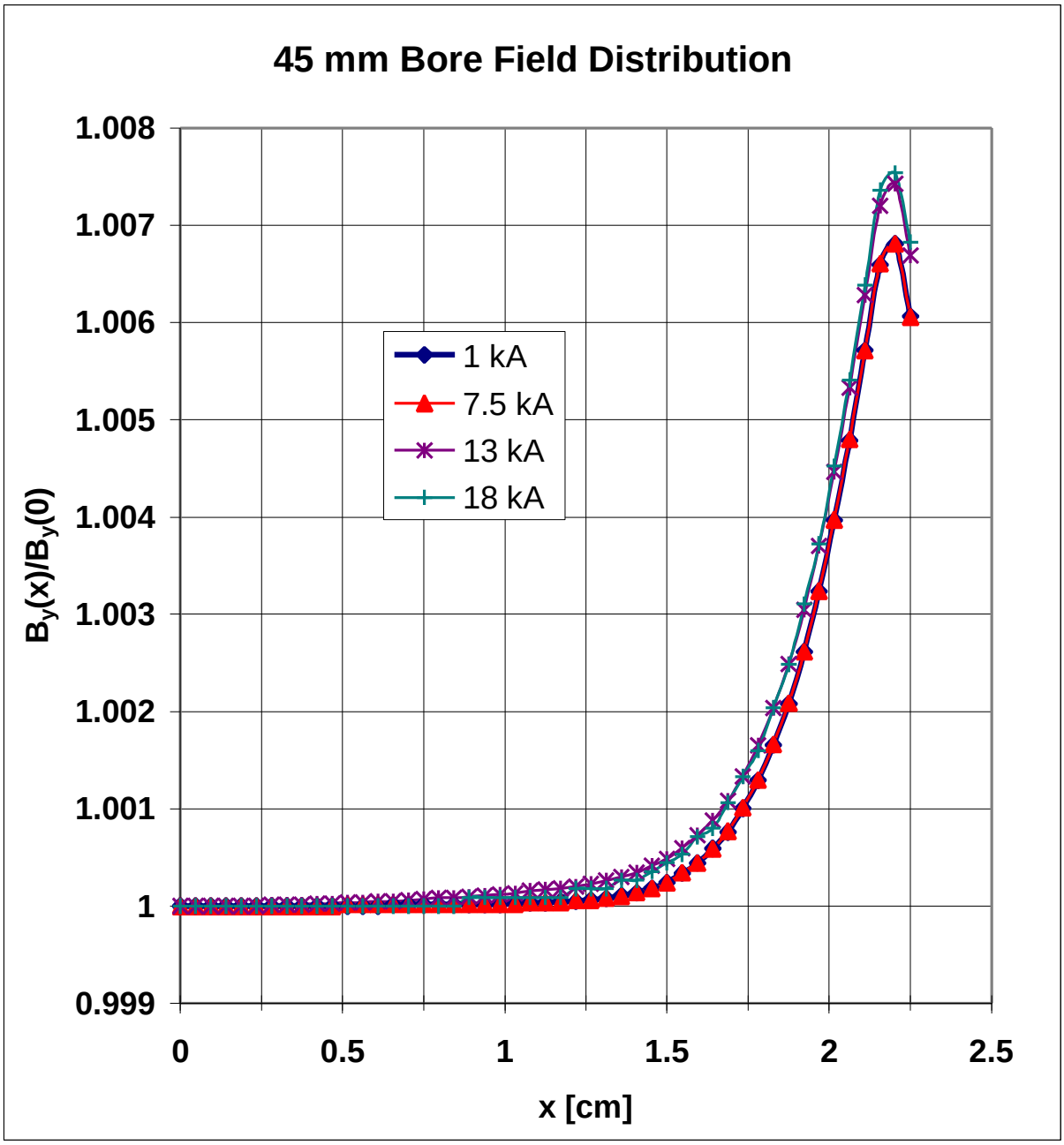

Figure 4. $B_y(x)$ Field distribution on the median plane for the magnet with 25 mm thick collar and holes in the yoke.

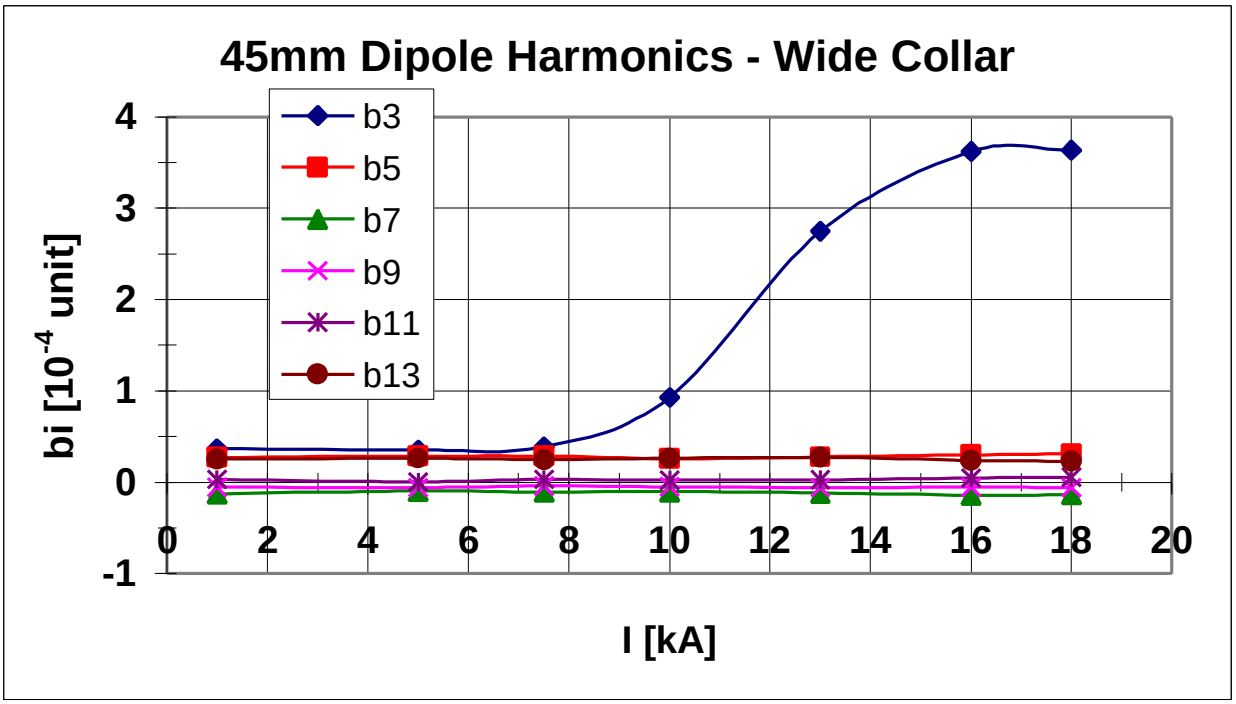

Figure 5a. Harmonics distribution for the thick-collared design without yoke holes.

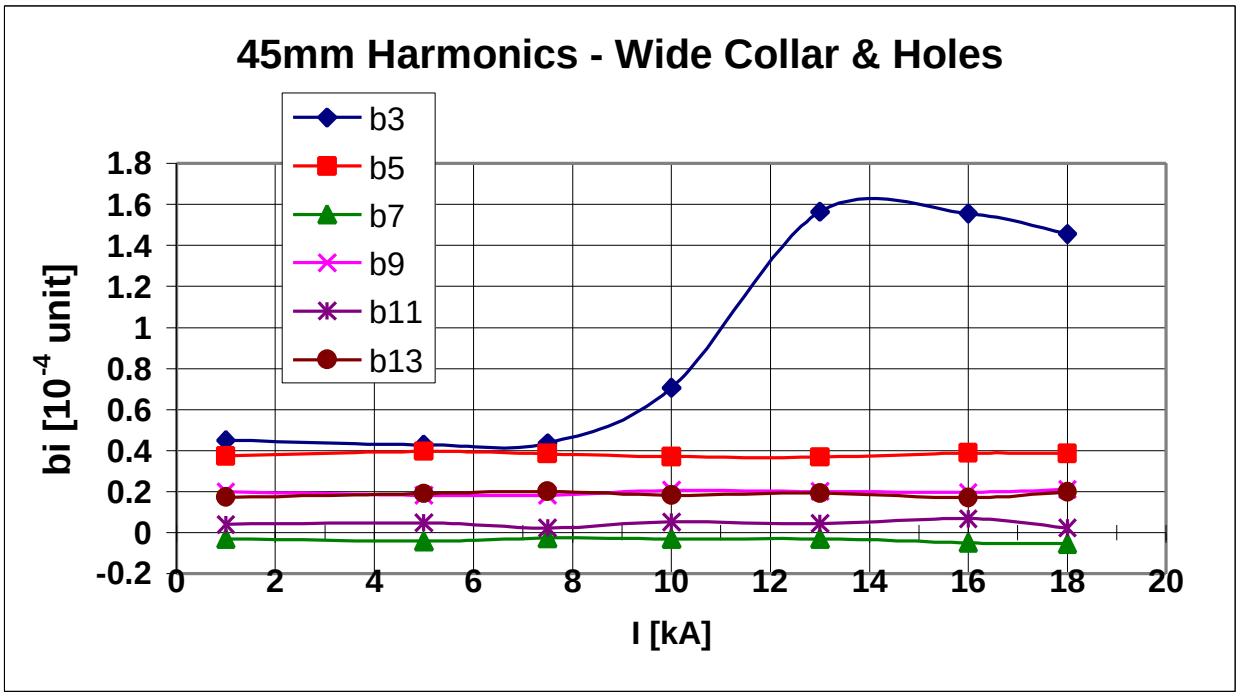

Figure 5b. Harmonics distribution for the thick-collared design with yoke holes.

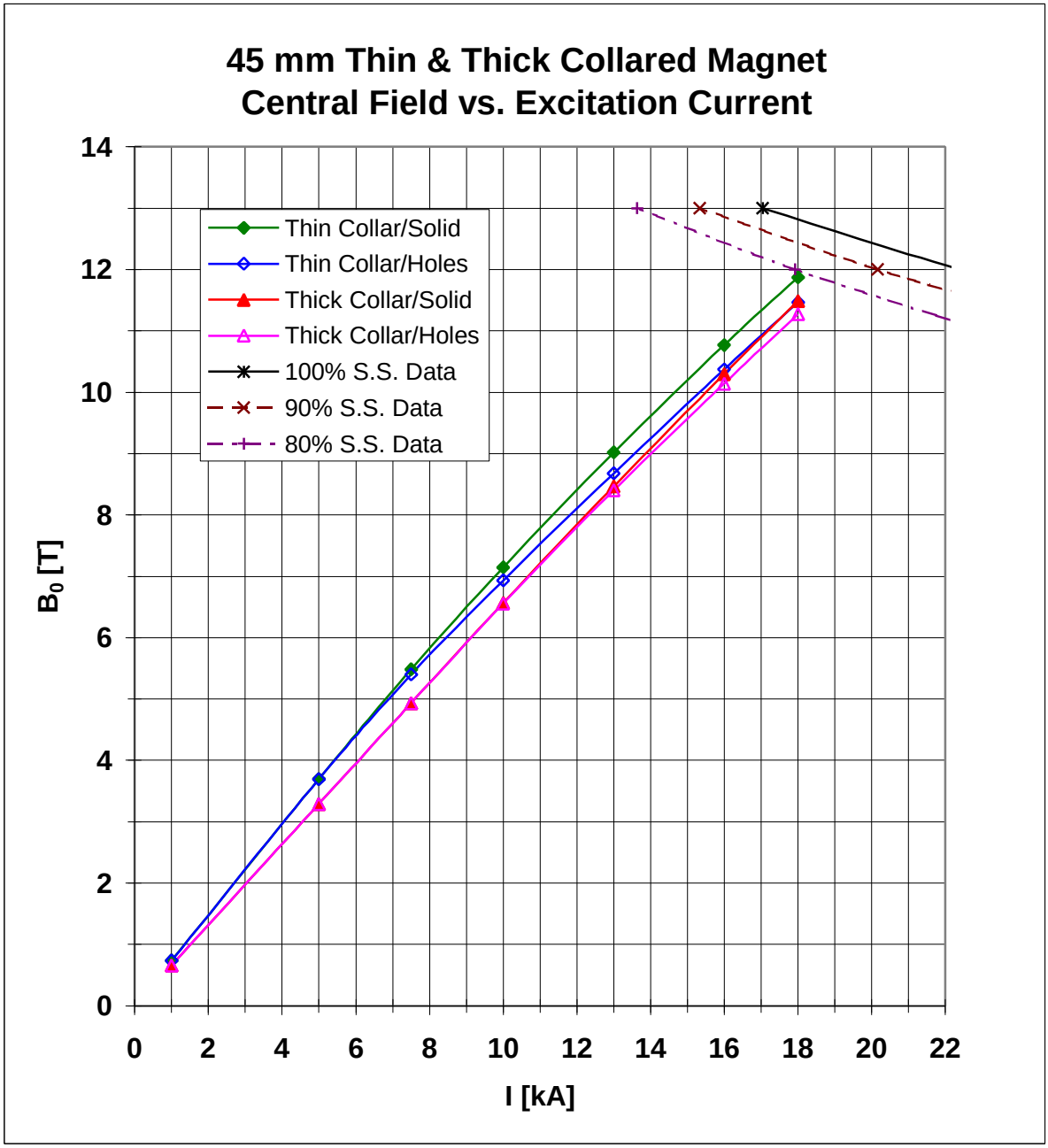

Figure 6a. The excitation curves of the 9 mm spacer and 25 mm thick collar designs. Data are shown for both designs with and without saturation correction holes.

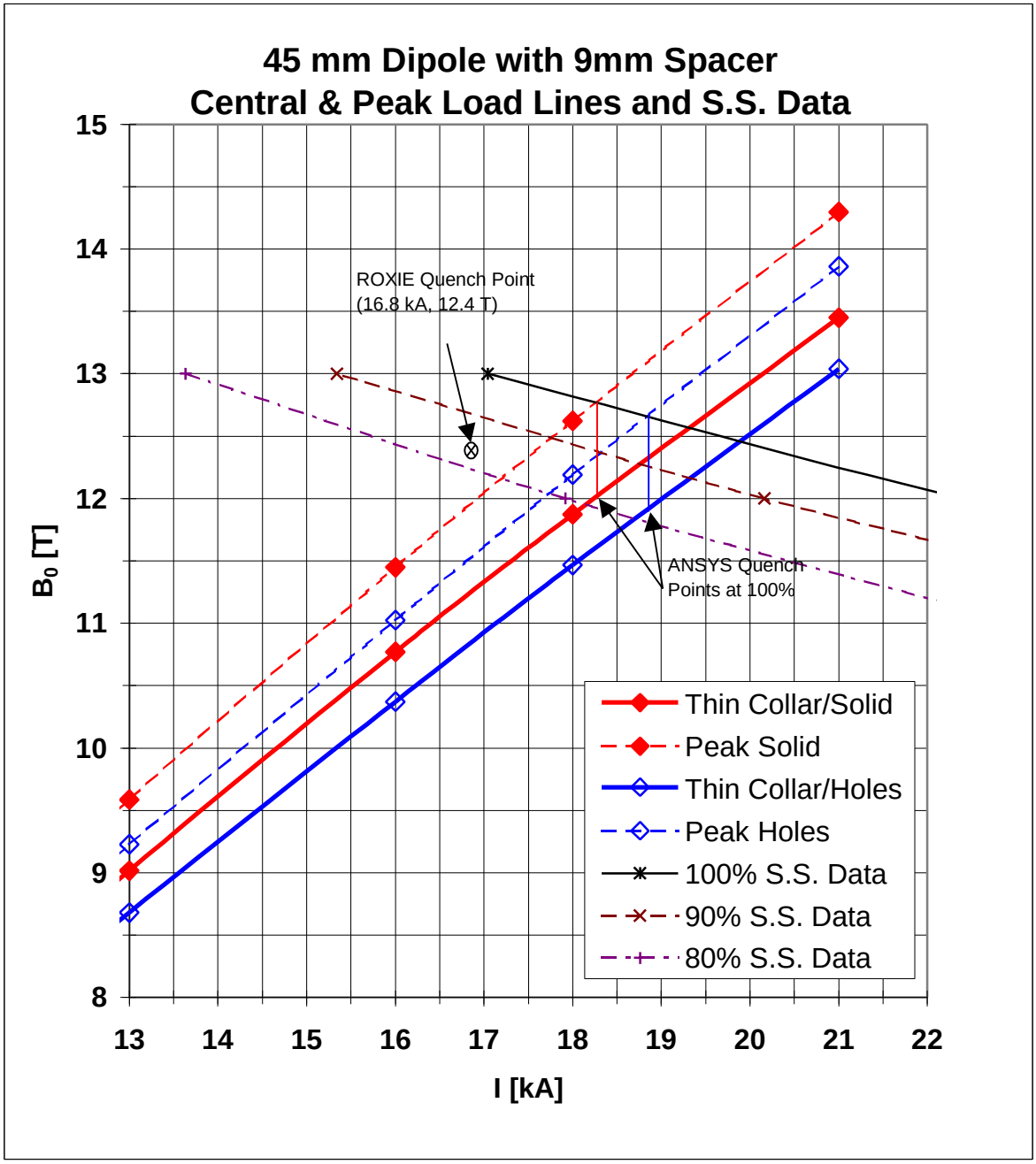

Figure 6b. Load lines and maximum attainable field values for the 9 mm spacer design

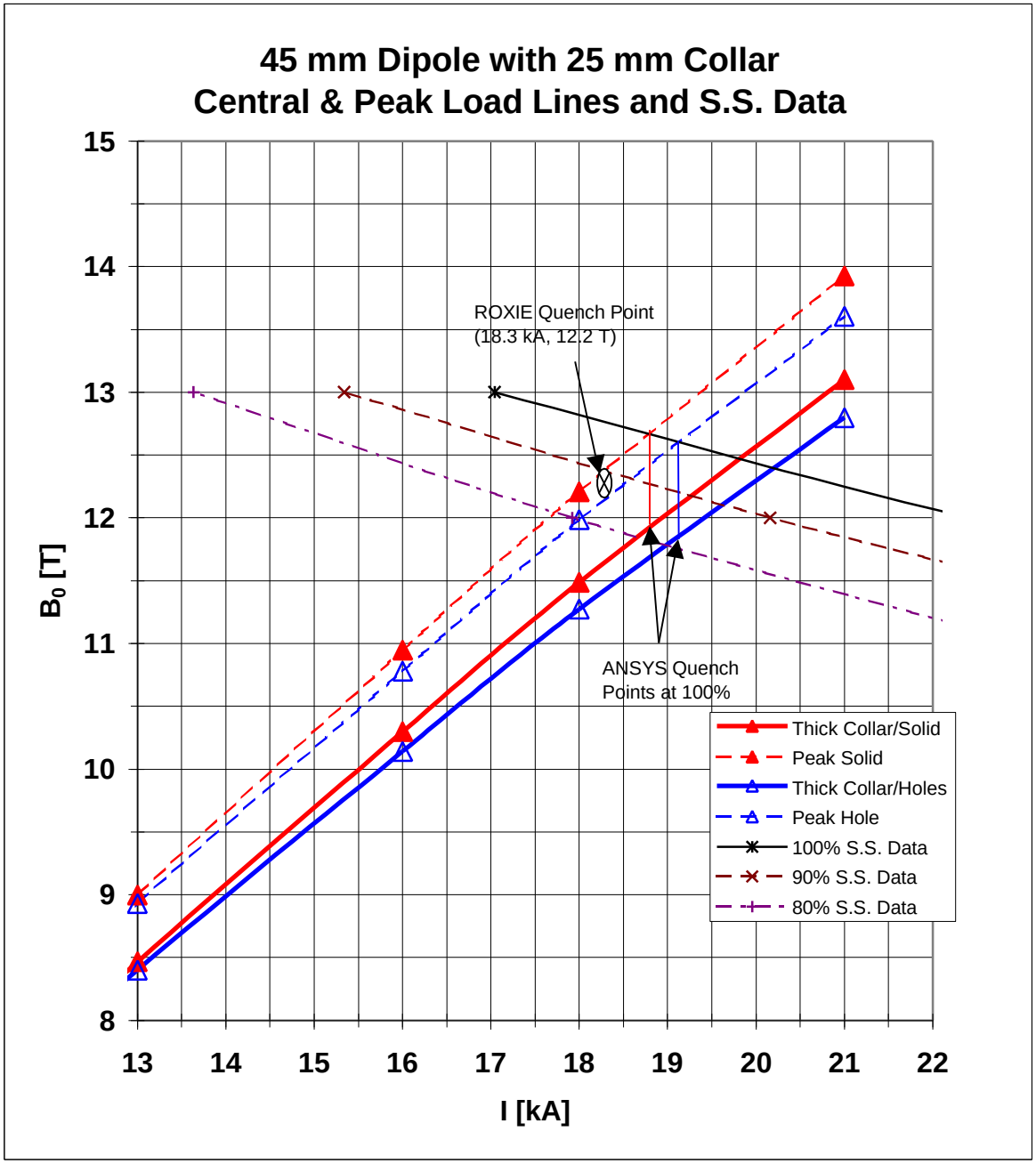

Figure 6c. Load lines and maximum attainable field values for the 25 mm collared design.

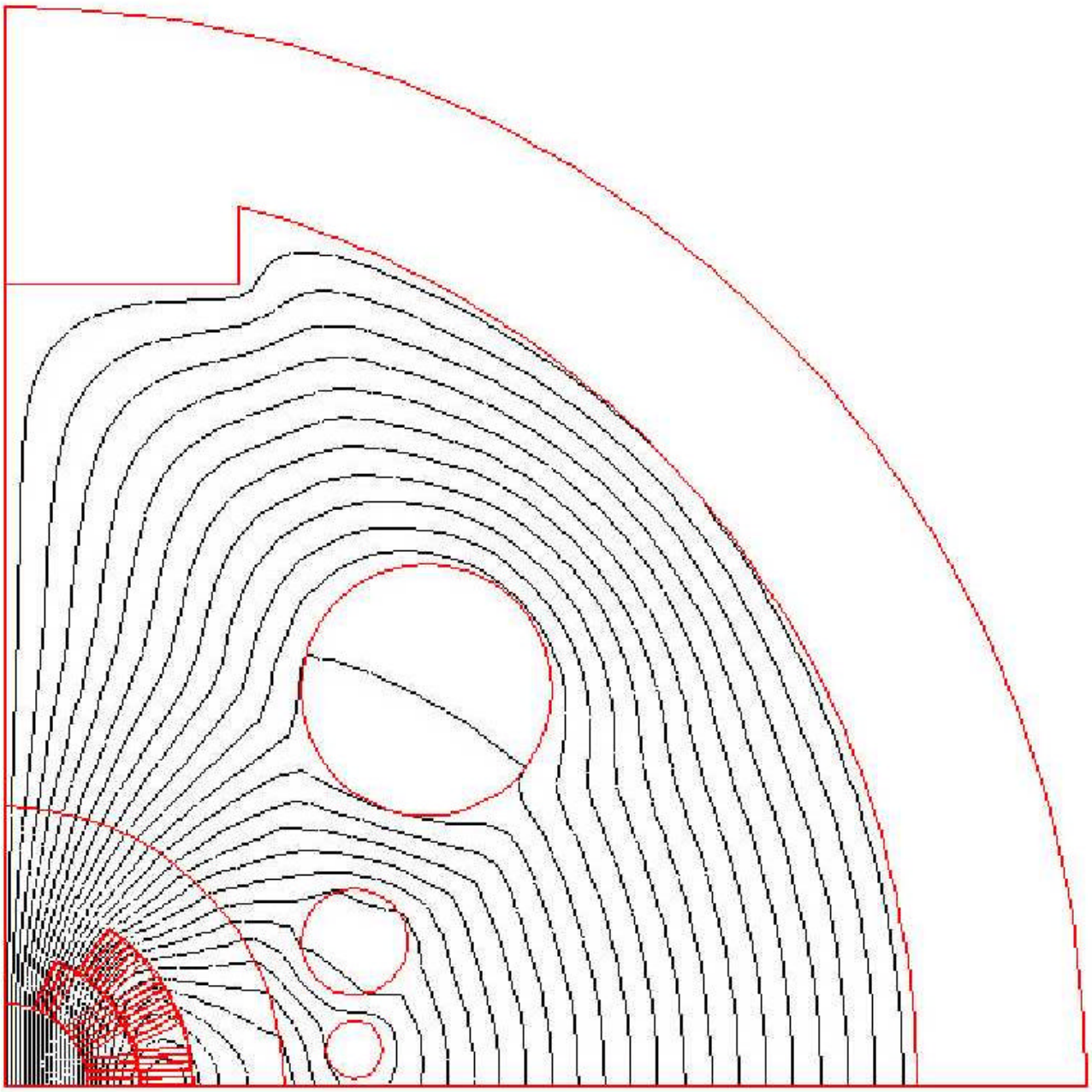

Figure 7. Geometry of the 25 mm thick-collared magnet with holes for saturation correction. Flux distribution is shown at an excitation current of 18 kA. B_0 = 11.48 T.

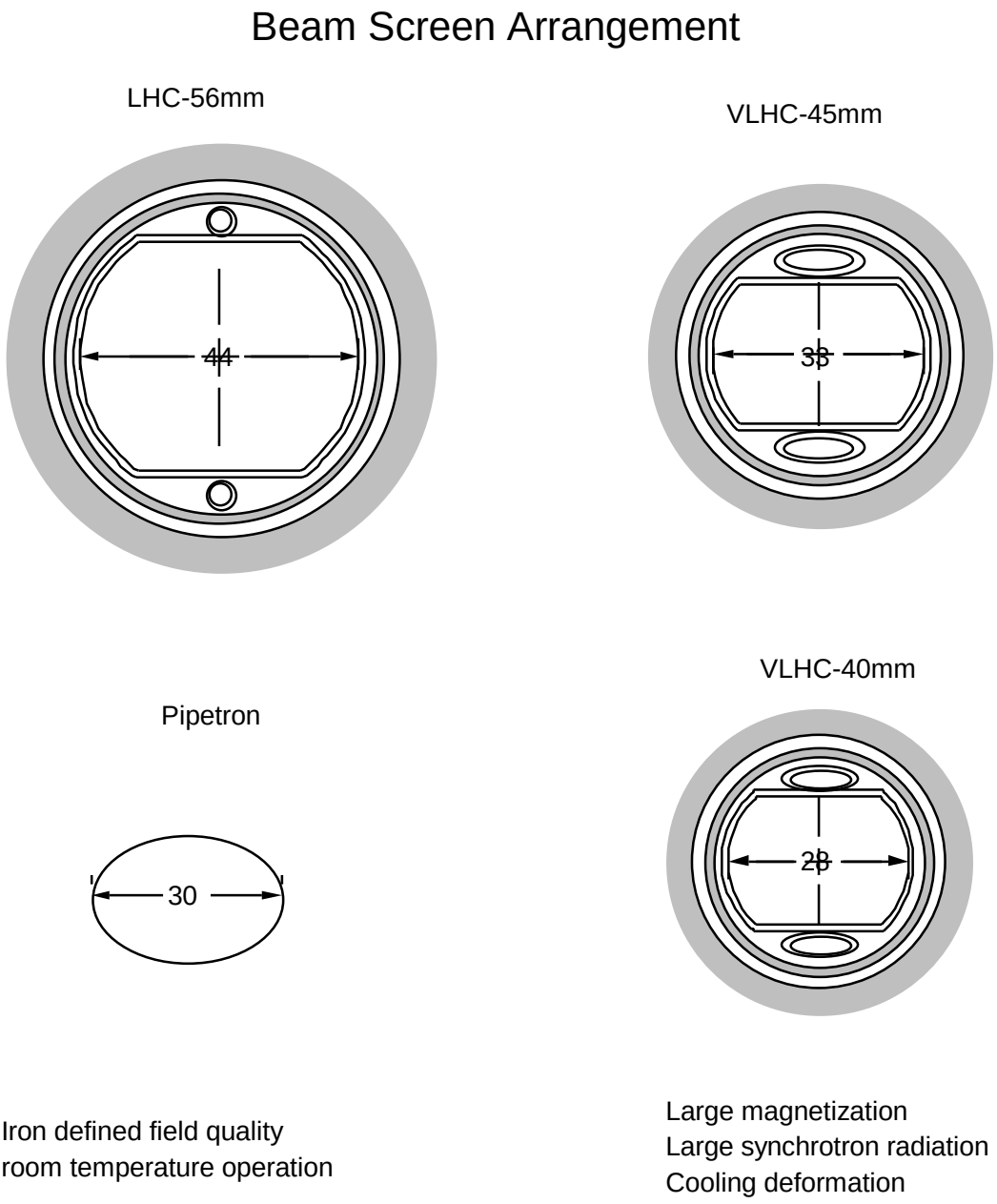

Figure 8. Various considerations for beam screen arrangement.

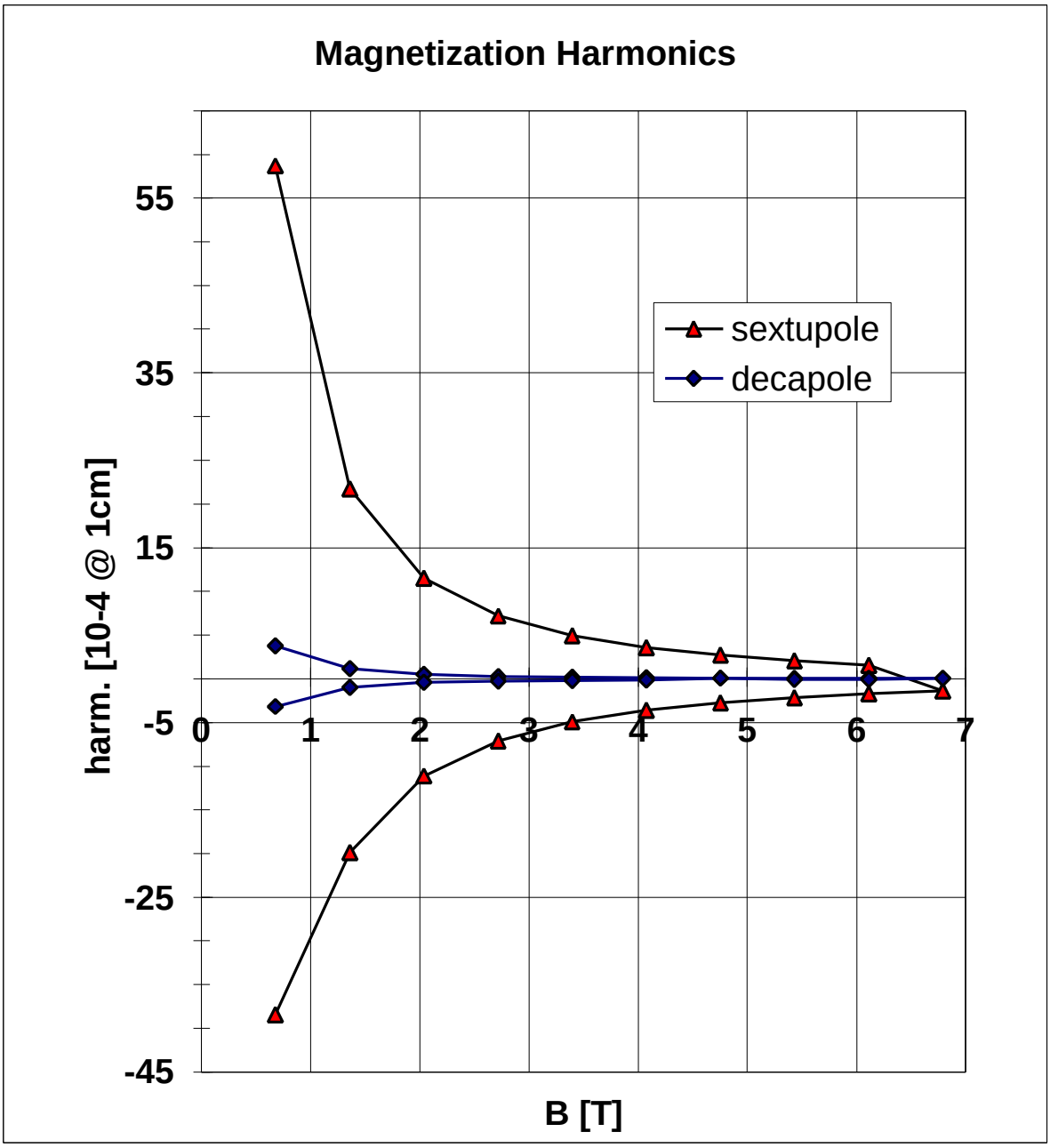

Figure 9. Magnetization Harmonics for 50-mm Bore Magnet with 70 mm Filaments.